Low-temperature transport, optical, magnetic and thermodynamic properties of $Fe_{1-x}Co_xSi$

M. A. Chernikov, L. Degiorgi, E. Felder, S. Paschen, A. D. Bianchi, and H. R. Ott
Laboratorium für Festkörperphysik, Eidgenössische Technische Hochschule-Hönggerberg, CH-8093 Zürich, Switzerland

J. L. Sarrao and Z. Fisk
National High Magnetic Field Laboratory, Florida State University, 1800 East Paul Dirac Drive, Tallahassee, Florida 32306

D. Mandrus*
Los Alamos National Laboratory, Los Alamos, New Mexico 87545
(Received 24 January 1997)

We report measurements of the electrical conductivity $\sigma(T)$, the optical reflectivity $R(\omega,T)$, the low-field ac magnetic susceptibility $\chi'(T,f)$, and the specific heat $C_p(T)$ for polycrystalline samples of $Fe_{1-x}Co_xSi$ with $0 \leqslant x \leqslant 0.03$ at low temperatures. Between 130 and 300 K the temperature variation of $\sigma(\omega,T)$ is consistent with that of a hybridization-gap semiconductor and is very similar for all samples. Below 50 K $\sigma(0,T)$ strongly depends on the cobalt concentration x and $d\sigma/dT$ decreases with decreasing x, changing sign from positive to negative in the range $0.01 \leqslant x \leqslant 0.02$. For $x \leqslant 0.0075$ the dc conductivity σ tends to saturate below 0.1 K, indicating a semimetallic regime characterized by a very low density of itinerant carriers. For $x \geqslant 0.01$ the $\chi'(T)$ curves show maxima at different temperatures $T_f(x)$ manifesting a spin-glass-type freezing of magnetic moments below 1 K. The small values of T_f/x and the frequency dependences of T_f both suggest a weak magnetic interaction. The low-temperature specific heat $C_p(T)$ contains a term γT that increases with increasing x from $2.1T$ mJ mol^{-1} K^{-1} for pure FeSi to $7.6T$ mJ mol^{-1} K^{-1} for $Fe_{0.97}Co_{0.03}Si$. Together with the results of the optical measurements this implies a respectable low-temperature mass enhancement of the itinerant carriers on the order of 30. [S0163-1829(97)04027-7]

I. INTRODUCTION

FeSi is a cubic narrow-gap semiconductor (space group $P2_13$) that has been claimed to share common features with a class of rare-earth compounds known as hybridization-gap semiconductors or Kondo insulators.[1] The magnetic susceptibility $\chi(T)$ of FeSi shows a maximum at about 500 K and an activated behavior below that temperature corresponding to a narrow gap in the excitation spectrum.[2] No magnetic order or spin-glass freezing occurs in this material, at least down to 0.04 K.[3] At very low temperatures the electrical conductivity of FeSi is very low but metallic in character.[3–5] Its isostructural counterpart CoSi is a diamagnetic semimetal with a temperature-independent susceptibility.[6] The nature of the gap in the excitation spectrum of FeSi remains an open issue of debate from both the experimental and theoretical points of view. In fact, for some aspects of the results of $\sigma(T)$ and $\chi(T)$ measurements, difficulties in interpretation with theoretical calculations still exist.[7–10] Furthermore, there is evidence for a possible difference between gaps in the charge and spin excitation channels, respectively.[10]

Previous investigations have shown that the transport properties of FeSi are very much affected by replacing Fe by Co.[11,12] With the aim to learn more about the ground state of FeSi we set out to study in more detail the question of possible consequences of Co doping on electronic and thermal properties, considering both itinerant and localized charge carriers. In addition, optical measurements were included to reveal details of the electronic excitation spectrum and a possible interplay between electronic and lattice excitations.

Below we report the results of this investigation of some low-temperature electrical-transport, optical, magnetic, and thermodynamic properties of pure and Co-doped FeSi. $Fe_{1-x}Co_xSi$ forms disordered solid solutions with the $B20$ structure at all x. This system exhibits two critical concentrations $x_1 = 0.05$ and $x_2 = 0.8$ for the onset of an inhomogeneous long-period helimagnetic order, tentatively attributed to a Dzyaloshinsky–Moriya spin-orbit-type coupling, which can occur in the noncentrosymmetric $B20$ structure.[13–15] The occurrence of a long-period helimagnetic order has previously been reported for the related $B20$ transition-metal compounds MnSi (Ref. 16) and FeGe (Ref. 17).

II. SAMPLES AND EXPERIMENTS

Polycrystalline ingots of $Fe_{1-x}Co_xSi$ with Co concentrations in the range $0 \leqslant x \leqslant 0.03$ were prepared by melting together appropriate quantities of constituents in an rf furnace. Our samples, with dimensions of approximately $1.5 \times 1.5 \times 5$ mm, were cut from the ingots using spark erosion.

The electrical conductivity, the optical reflectivity, the ac magnetic susceptibility, and the specific heat were measured in varying ranges of temperature between 0.05 and 300 K. For each concentration of cobalt, all measurements reported below were done using the *same* sample. This matter is particularly important in the case of FeSi, the composition of which can vary from 49 to 50.5 at.% Si.[18]

The electrical conductivity was measured by a standard low-frequency ac four-probe technique in the temperature range between 0.05 and 300 K. The samples were fixed to a heat sink with a thin layer of GE-7031 varnish at one end to

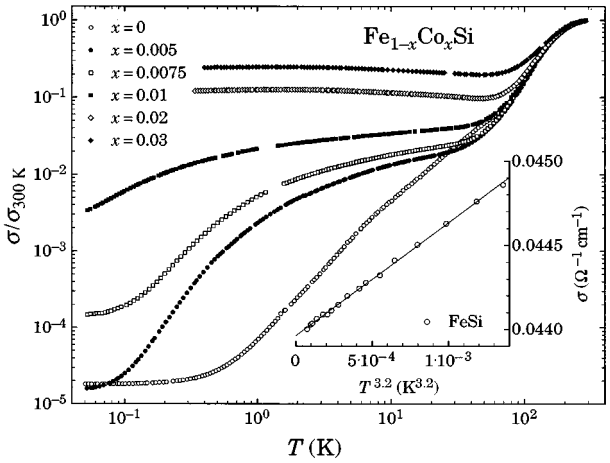

FIG. 1. The electrical conductivity σ of $Fe_{1-x}Co_xSi$ plotted as $\sigma/\sigma_{300\,K}$ vs T between 0.05 and 300 K on a log-log scale. The inset shows the conductivity σ of nominally pure FeSi plotted as a function of $T^{3.2}$, below 0.17 K.

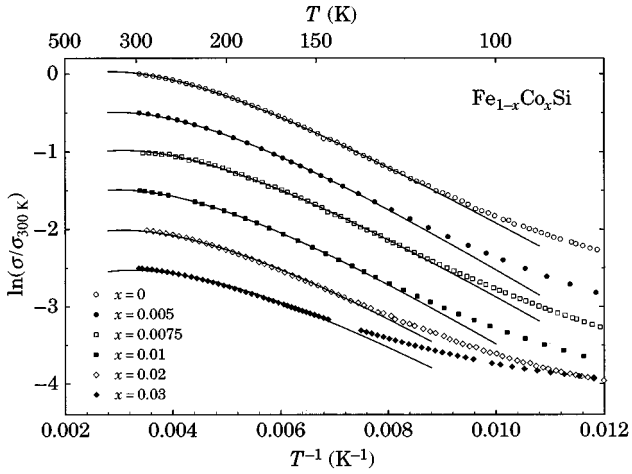

FIG. 2. The conductivity data $\sigma(T)$ of $Fe_{1-x}Co_xSi$ between 80 and 300 K plotted as $\ln(\sigma/\sigma_{300\,K})$ vs T^{-1}. The data of different samples are shifted along the vertical axis by 0.5 for clarity. The lines are fits of Eq. (2) to the data of $Fe_{1-x}Co_xSi$ in the region 130–300 K.

reduce the cooling-induced stress.[3]

The low-frequency and low-field ac magnetic susceptibility data were obtained with a conventional mutual-inductance technique in varying temperature ranges between 0.05 and 4 K. Measurements were made in the frequency range between 18 and 630 Hz and with an excitation-field amplitude in the range from 0.025 to 0.1 Oe. The signal of the pickup coil was measured with a two-channel lock-in amplifier monitoring simultaneously the in-phase χ' and the out-of-phase component χ''. A low-noise signal transformer was used to match the impedances of the pick-up coil and the lock-in amplifier.

The specific heat $C_p(T)$ was measured using a relaxation-type method in the temperature range between 0.05 and 31 K. The temperatures in the range between 0.05 and 1 K were reached in a dilution refrigerator. Conventional ^{3}He and ^{4}He cryostats were used for temperatures between 0.35 and 4 K, and above 1.5 K, respectively.

The optical reflectivity $R(\omega)$ of $Fe_{1-x}Co_xSi$ has been measured for the samples with $x = 0$, 0.005, 0.02, and 0.03 in the frequency range between 15 and 10^5 cm^{-1}, i.e., over almost 4 orders of magnitude in frequency and at selected fixed temperatures. The optical conductivity $\sigma_1(\omega)$ was obtained by performing a Kramers-Kronig transformation of the reflectivity $R(\omega)$ spectra extrapolated to lower and higher frequencies. Details concerning the experimental setup and the extrapolation procedure can be found in Ref. 19.

III. RESULTS, ANALYSIS, AND DISCUSSION

A. Electrical conductivity

The electrical conductivity $\sigma(T)$ of polycrystalline samples of $Fe_{1-x}Co_xSi$ was measured in the temperature range between 0.05 and 300 K for $0 \leqslant x \leqslant 0.01$ and between 0.4 and 300 K for $0.02 \leqslant x \leqslant 0.03$. The room-temperature conductivities $\sigma_{300\,K}$ of the investigated materials fall into the range between 1.5×10^3 and 4×10^3 $\Omega^{-1}\,cm^{-1}$. Our electrical-conductivity data are shown in Fig. 1 as a log-log plot of $\sigma/\sigma_{300\,K}$ versus T. Part of the same data for temperatures between 80 and 300 K are plotted as $\ln(\sigma/\sigma_{300\,K})$ versus T^{-1} and displayed in Fig. 2.

We first analyze the conductivity behavior for nominally pure FeSi. We note that although $\sigma(T)$ was measured on a polycrystalline sample, the general features are very close to those revealed in experiments using single crystals.[5] Below 300 K, there is a monotonic drop in conductivity by almost five orders of magnitude to the lowest measured temperature of 0.05 K. Between 200 and 300 K, the $\ln(\sigma/\sigma_{300\,K})$ versus T^{-1} curve tends to level off with increasing temperature, indicating that the material enters the electronically degenerate regime. In the whole temperature range measured we are not able to identify a regime of thermally activated conductivity

$$\sigma \propto \exp\left(-\frac{E_{gap}}{2k_BT}\right) \tag{1}$$

over any extended range of temperature because the temperature variation of σ is, strictly speaking, characterized by a temperature dependent slope $d\ln\sigma/d(T^{-1})$.

It has previously been shown[20,10] that above 100 K the behavior of σ of pure FeSi is consistent with that of a hybridization-gap semiconductor, i.e., a system with a strong renormalization of the noninteracting bands and their widths that leads to an enhanced electronic density of states (DOS) at the gap edges. While an applicability of a hybridization-gap-semiconductor approach to FeSi may be questioned on general grounds, it seems to consistently describe magnetic, thermodynamic, and transport properties of this material at temperatures exceeding 100 K.[20,10] In addition, high-resolution angle-resolved photoemission studies of FeSi (Refs. 21 and 22) have shown the development of a band with spectacularly sharp features near the upper edge of the valence band, which strongly supports a picture involving two narrow bands at the edges of a narrow gap.

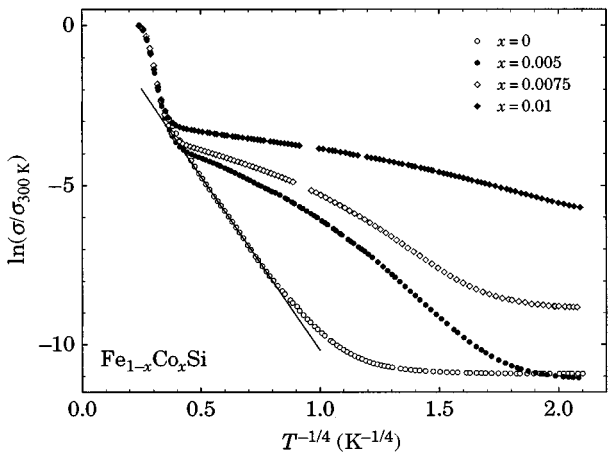

FIG. 3. $\ln(\sigma/\sigma_{300\,\mathrm{K}})$ vs $T^{-1/4}$ of $Fe_{1-x}Co_xSi$ with $0 \leqslant x \leqslant 0.01$ in the temperature range 0.05–300 K. The line is a fit of Eq. (3) to the $\sigma(T)$ data of pure FeSi between 2.5 and 20 K.

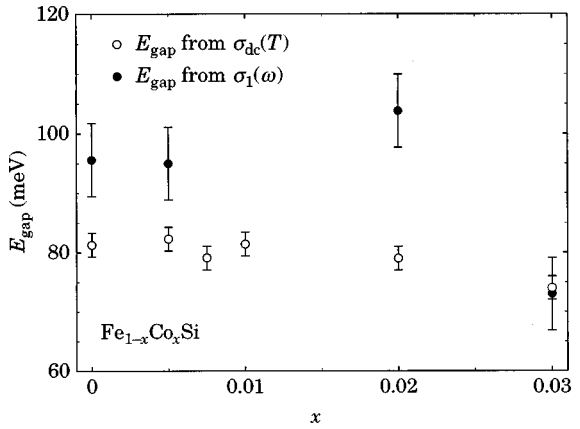

FIG. 4. Energy gap E_{gap} as a function of cobalt concentration x obtained from fitting Eq. (2) to the $\sigma(T)$ data of $Fe_{1-x}Co_xSi$ between 130 and 300 K (open circles) and from the optical conductivity $\sigma_1(\omega)$ (closed circles).

The assumptions that the electronic DOS can be approximated by two rectangular bands, each of width W, separated by an energy gap E_{gap} and that the mobility b of the itinerant charge carriers is limited by electron-phonon scattering; i.e., $b \propto T^{-3/2}$, leads to

$$\sigma \propto T^{-3/2}\left\{1-\frac{k_BT}{W}\ln\left[1+\exp\left(\frac{E_{gap}+2W}{2k_BT}\right)\right]+\frac{k_BT}{W}\ln\left[1+\exp\left(\frac{E_{gap}}{2k_BT}\right)\right]\right\}. \quad (2)$$

Here it is also assumed that the chemical potential μ resides in the center of the energy gap and is temperature independent, which is consistent with electron-hole symmetry of the model DOS.[10] These assumptions are expected to be valid at not too low temperatures, i.e., in the temperature range of the intrinsic regime. A fit of Eq. (2) to $\sigma(T)$ of pure FeSi in the temperature range between 130 and 300 K, shown in Fig. 2 as the solid line through the data points of FeSi, yields $E_{gap}=81$ meV and $W=39$ meV, in fair agreement with analogous values reported in Refs. 20 and 10.

On the log-log scale used in Fig. 1 one recognizes a shoulder in the electrical conductivity data at $T \approx 80$ K. Below that temperature σ drops further with decreasing T but tends to saturate below 1 K, reaching $4.4\times10^{-2}\ \Omega^{-1}\,\mathrm{cm}^{-1}$ at 0.05 K. Nowhere in this regime is it possible to describe the data with a thermally activated behavior over any extended temperature range.

In previous studies of FeSi (Ref. 23) it has been claimed that in the limited range of temperatures between 2.5 and 40 K, $\sigma(T)$ of pure FeSi can be described with a variable-range-hopping behaviour,[24] i.e.,

$$\sigma \propto \exp\left[-\left(\frac{T_{1/4}}{T}\right)^{1/4}\right]. \quad (3)$$

A fit of Eq. (3) to our $\sigma(T)$ data of pure FeSi in the temperature range 2.5–20 K shown in Fig. 3 yields $T_{1/4}=1.43\times10^4$ K, which is very close to the $T_{1/4}$ value of 1.42×10^4 K reported in Ref. 23. For samples with $x \neq 0$, however, it may be seen that this type of approximation is not appropriate.

At the lowest temperatures below 0.18 K, the conductivity σ is well described by an expression of the form

$$\sigma = \sigma_0 + mT^{\alpha}, \quad (4)$$

as shown in the inset of Fig. 1. In this regime we find $\sigma_0=4.4\times10^{-2}\ \Omega^{-1}\,\mathrm{cm}^{-1}$, $m=0.72\ \Omega^{-1}\,\mathrm{cm}^{-1}\,\mathrm{K}^{-3.2}$, and $\alpha=3.2$. We note that the value of the exponent α is very large compared with $\alpha \sim 2$ previously reported for metallic samples of doped semiconductors close to the metal to nonmetal transition.[25]

We now focus on the $\sigma(T)$ variation of Co-doped FeSi. Between 90 and 300 K, $\sigma(T)$ of these samples is qualitatively similar to that of nominally pure material. Between 130 and 300 K the conductivity σ is again well described by Eq. (2) appropriate for a hybridization-gap semiconductor in the regime of intrinsic conductance (see Fig. 2). The energy gap E_{gap} that follows from the analysis of our $\sigma(T)$ data for $Fe_{1-x}Co_xSi$ appears to be independent of the cobalt concentration x for materials with $x \leqslant 0.02$ and it slightly decreases with further increasing x (see Fig. 4).

Below 90 K $\sigma(T)$ depends strongly on the doping level. In the $\log_{10}(\sigma/\sigma_{300\,\mathrm{K}})$ versus $\log_{10}T$ plot shown in Fig. 1, the curves are seen to become less steep with increasing x. Below about 30 K, $\sigma/\sigma_{300\,\mathrm{K}}$ of $Fe_{0.995}Co_{0.005}Si$ is noticeably higher than that of nominally pure FeSi, the difference amounting to $1\frac{1}{2}$ orders of magnitude at 1 K. Below 1 K, where σ of pure FeSi saturates, the conductivity of $Fe_{0.995}Co_{0.005}Si$ keeps dropping steeply with decreasing T until it tends to saturate below 0.15 K, reaching a level, that is close to that of pure FeSi in this temperature range. The samples with $x=0.0075$ and 0.01 show a $\sigma(T)$ variation, which is qualitatively similar to that of $Fe_{0.995}Co_{0.005}Si$ but their conductivities at $T=0.05$ K are higher than that of $Fe_{0.995}Co_{0.005}Si$ by one and two orders of magnitude, respectively.

For Co-doped FeSi we were not able to identify regimes of thermally activated conductivity or of variable-range hop-

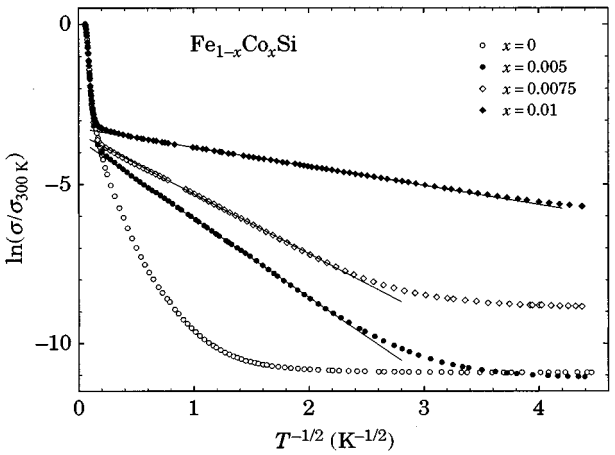

FIG. 5. $\ln(\sigma/\sigma_{300\,\mathrm{K}})$ vs $T^{-1/2}$ of $Fe_{1-x}Co_xSi$ with $0 \leqslant x \leqslant 0.01$ between 0.05 and 300 K. Lines indicate fits of the $\sigma(T)$ data of the Co-doped materials using Eq. (5) in the temperature range between 0.2 and 4 K.

ping over any extended range of temperature below 90 K. However, we note that an expression of the form

$$\sigma \propto \exp\left[-\left(\frac{T_{1/2}}{T}\right)^{1/2}\right] \tag{5}$$

appropriate for a regime of variable-range hopping in the presence of a Coulomb gap,[26,27] i.e., when the single-particle density of states close to the chemical potential is depleted due to the Coulomb interaction between electrons, seems to describe our conductivity data for $Fe_{1-x}Co_xSi$ with $0.005 \leqslant x \leqslant 0.01$ over substantial temperature ranges (see Fig. 5).

With increasing x the conductivity saturation at very low temperatures that dominates the $\sigma(T)$ data of nominally pure FeSi becomes less pronounced and it is not well developed in the conductivity data of $Fe_{0.99}Co_{0.01}Si$. The saturation trend of σ at low temperatures may be described qualitatively using an approach based on an evaluation of the derivative $d\ln\sigma/d\ln T$.[28] This simple but instructive analysis is meant to allow for the identification of the type of conductivity from the $d\ln\sigma/d\ln T$ behavior at low temperatures. In the metallic regime σ approaches nonzero values as T tends to zero and therefore $d\ln\sigma/d\ln T \to 0$ as $T \to 0$. If σ follows an exponential temperature dependence as, e.g., in the variable-range-hopping regime, $d\ln\sigma/d\ln T$ diverges at zero temperature. Finally, for many-electron cascade transitions in the insulating regime, σ is expected to vary as T^s with $s \gg 1$.[29] In this case, $d\ln\sigma/d\ln T$ would tend to a constant nonzero value for $T \to 0$.

We have calculated the numerical derivative $d\ln\sigma/d\ln T$ using $\sigma(T)$ of our $Fe_{1-x}Co_xSi$ samples. The results of this calculation are plotted versus $\ln T$ in Fig. 6. The peak between 100 and 200 K common to all samples reflects the crossover between the regimes of intrinsic and extrinsic conduction. According to this analysis of $d\ln\sigma/d\ln T$, pure FeSi clearly exhibits metallic behavior at low temperatures. For $Fe_{1-x}Co_xSi$ with $0.005 \leqslant x \leqslant 0.01$, $d\ln\sigma/d\ln T$ first increases with decreasing temperature below 10 K and after reaching a maximum at a temperature, which depends on x, decreases

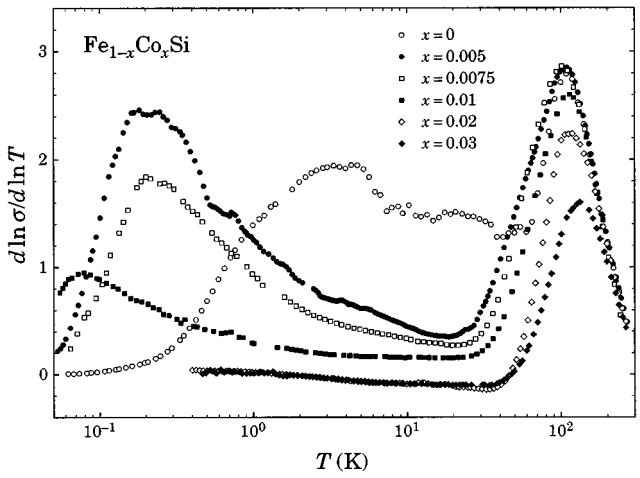

FIG. 6. $d\ln\sigma/d\ln T$ vs $\log_{10}T$ of $Fe_{1-x}Co_xSi$.

with further decreasing T. Although for the samples with $0.005 \leqslant x \leqslant 0.01$ $d\ln\sigma/d\ln T$ is still nonzero at the lowest temperatures of 0.05 K reached in our experiments, the positive slope of the $d\ln\sigma/d\ln T$ versus $\log_{10}T$ curves close to $T = 0.05$ K suggests that all these samples are metallic as $T \to 0$. Below 0.08 K the electrical conductivity $\sigma(T)$ of $Fe_{1-x}Co_xSi$ with $0.005 \leqslant x \leqslant 0.01$ can be well described by Eq. (4). The fitted values of the parameters σ_0 and α are plotted in Fig. 7 as functions of cobalt concentration x.

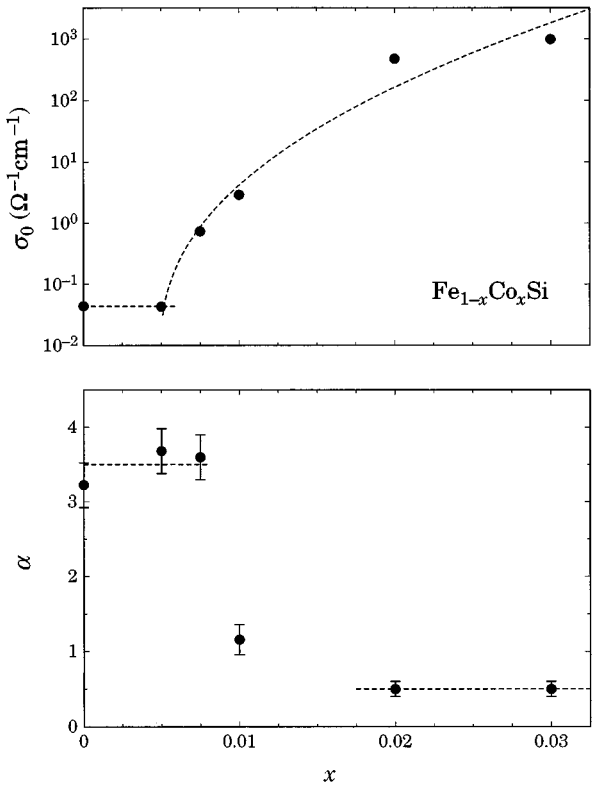

FIG. 7. Zero-temperature conductivity σ_0 and the exponent α obtained from fitting Eq. (4) to the $\sigma(T)$ data of $Fe_{1-x}Co_xSi$ plotted as functions of cobalt concentration x. The fitting ranges are 0.05–0.08 K and 0.35–0.5 K for $0 \leqslant x \leqslant 0.01$ and $0.02 \leqslant x \leqslant 0.03$, respectively. The lines are guides for the eye.

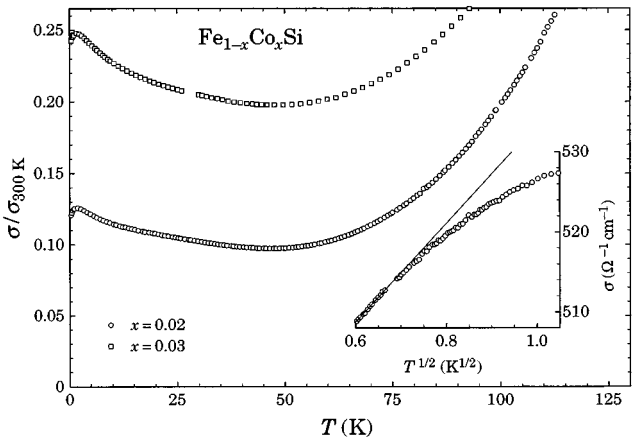

FIG. 8. $\sigma/\sigma_{300\,\mathrm{K}}$ vs T of $Fe_{1-x}Co_xSi$ with $x=0.02$ and 0.03 in the temperature range 0.35–100 K. The inset shows σ of $Fe_{0.98}Co_{0.02}Si$ as a function of $T^{1/2}$ between 0.35 and 1 K.

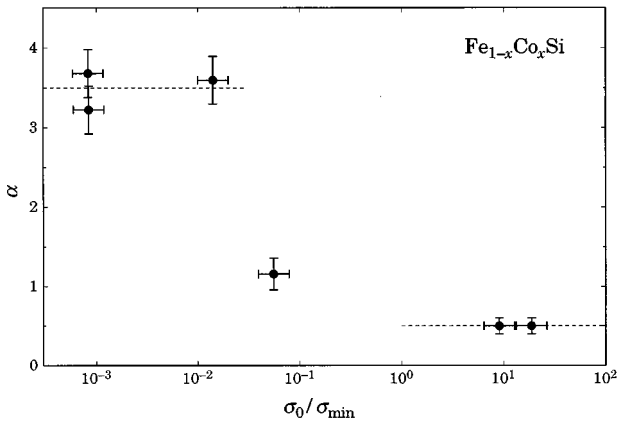

FIG. 9. Power-law exponent α vs $\sigma_0/\sigma_{\min}$. Here we used $\sigma_{\min}=52\ \Omega^{-1}\,\mathrm{cm}^{-1}$ calculated for $C_3=0.035$. The horizontal error bars are meant to indicate an uncertainty in the choice of C_3, which lies in the range between 0.025 and 0.05 (see text). The lines are guides for the eye.

For Co concentrations $x=0.02$ and 0.03, the conductivity σ depends relatively weakly on temperature below 90 K (see Fig. 8). Here σ first decreases with decreasing T, reaches a shallow minimum at approximately 50 K, and then increases with further decreasing temperature with a very small negative slope $d\sigma/dT$. For both samples, the slope $d\sigma/dT$ again changes sign at $T\approx 1.5$ K and it remains positive down to the lowest measured temperature of 0.4 K. Well below 1 K, the electrical conductivity $\sigma(T)$ is adequately fitted using Eq. (4) with $\alpha\approx 0.5$ and $m\approx 60\ \ \Omega^{-1}\,\mathrm{cm}^{-1}\,\mathrm{K}^{-1/2}$ (see inset of Fig. 8). This implies that the temperature dependence of the conductivity $\sigma(T)$ of $Fe_{1-x}Co_xSi$ with $x=0.02$ and 0.03 close to $T=0$ is determined by the diffusion-channel term characteristic of disordered metals with low electron diffusivity. The diffusion-channel correction to the classical Boltzmann conductivity arises from quantum-interference effects when the scattering is predominantly elastic, and it is due to the Coulomb interaction between itinerant electrons whose combined total momentum p is small compared with the Fermi momentum p_F.[30]

We now comment on the composition dependence of the zero-temperature conductivity σ_0 and the power-law exponent α obtained using Eq. (4) and shown in Fig. 7. With decreasing x from 0.03 to 0.005, σ_0 rapidly decreases by more than 4 orders of magnitude but it saturates below $x=0.005$. The saturation of the zero-temperature conductivity σ_0 for $x\leqslant 0.005$ suggests that an additional mechanism of conduction sets in at the level of $\sigma_0\sim 0.04\ \Omega^{-1}\,\mathrm{cm}^{-1}$ and we will comment on this observation later. For $0.02\leqslant x\leqslant 0.03$, i.e., well within the metallic regime, $\alpha\approx 0.5$, independent of x. With further decreasing x the exponent α increases rapidly, reaching 3.5 at $x=0.075$ and varying only weakly with x for $x\leqslant 0.075$. We note that positive and nonzero values of σ_0 confirm our conclusion, based on the analysis of $d\ln\sigma/d\ln T$, that all our samples of $Fe_{1-x}Co_xSi$ are metallic. Nevertheless, both the $\sigma_0(x)$ and the $\alpha(x)$ variation in the Co concentration range $0.005\leqslant x\leqslant 0.03$ are indicative of the proximity of a metal-to-insulator transition.

The assumptions that the composition-driven metal-to-insulator transition is bound to occur in $Fe_{1-x}Co_xSi$ with $x\approx 0.005$ and that the partial replacement of Fe by Co leads to one itinerant electron per cobalt impurity implies a minimum metallic conductivity $\sigma_{\min}$ given by[31]

$$\sigma_{\min}\approx C_3\frac{e^2}{\hbar\, l_{\min}}\approx 37-74\ \ \Omega^{-1}\,\mathrm{cm}^{-1}. \tag{6}$$

Here $l_{\min}$ is the shortest possible mean free path for which we take the mean separation between impurities, and C_3 lies in the range between 0.025 and 0.05. For $Fe_{1-x}Co_xSi$ with $x=0.005$ we calculate $l_{\min}\approx 17$ Å. In Fig. 9 we plot the power-law exponent α as a function of $\sigma_0/\sigma_{\min}$. We note that $\alpha\sim 0.5$ for $\sigma_0/\sigma_{\min}>1$ and $\alpha\sim 3.5$ when $\sigma_0/\sigma_{\min}$ is much less than unity (3 orders of magnitude). Apart from the somewhat large values of α at the lowest impurity concentrations x, the $\alpha(\sigma_0/\sigma_{\min})$ variation is in general agreement with what is usually observed on the metallic side of the metal to nonmetal transition of doped semiconductors.[25]

We note, however, that a transition to a nonmetallic state implies that σ_0 ought to decrease further with decreasing x below 0.005 and should vanish at a Co concentration x somewhat below 0.005, in obvious disagreement with our experimental results (see Fig. 7). A possible scenario that is consistent with our electrical conductivity $\sigma(T)$ data of $Fe_{1-x}Co_xSi$ is that below 0.1 K, FeSi enters a semimetallic regime characterized by a very low density of itinerant carriers as implied by the magnitude of σ_0.[5] This interpretation gains further support from a comparison of the temperature dependences of the conductivity in pure and moderately doped FeSi. While the values of the zero-temperature conductivity σ_0 of nominally pure FeSi and $Fe_{0.995}Co_{0.005}Si$ are almost equal, $\sigma(T)$ of these two materials varies in dramatically different ways at intermediate temperatures as shown in Fig. 1. Additionally, for pure FeSi the results of the ac conductivity measurements in the frequency range between 20 Hz and 1 GHz (Ref. 4) are consistent with an increase of the dielectric constant by an order of magnitude with decreasing temperature from 4 to 0.08 K, again suggestive of a metallic state. A further discussion on the density and mobility of

charge carriers in FeSi at low temperatures will be presented in a forthcoming publication.[32]

Taken together, the $\sigma(T)$ behavior of nominally pure and Co-doped FeSi is consistent with that of impure hybridization-gap semiconductors, for which in the intrinsic regime at high temperatures, the $\sigma(T)$ curves are expected to depend only slightly on doping. On the other hand, a strong concentration dependence of $\sigma(T)$ is expected in the regime of extrinsic conductance at low temperatures. The energy gap $E_{\rm gap}=81$ meV that follows from our $\sigma(T)$ data for nominally pure FeSi between 130 and 300 K is in fair agreement with our optical-conductivity results presented in Sec. III B and in Refs. 19 and 32, and also with the results of other experiments probing the width of the gap in the electronic excitation spectrum.[10,33–36]

Finally, we note that in the $Fe_{1-x}Co_xSi$ alloy series the transition from the regime of conductance characterized by a positive sign of $d\sigma/dT$ to the regime in which $d\sigma/dT$ is negative, occurring at Co concentrations x in the range between 0.01 and 0.02 at %, becomes manifest at temperatures just below the regime of intrinsic conductance. This is quite in contrast, for example, to antimony-doped germanium, for which an intermediate activation regime characterized by an activation energy E_1, has clearly been identified.[37]

B. Optical conductivity

Figure 10 presents $\sigma_1(\omega)$ at several selected temperatures for $Fe_{1-x}Co_xSi$ with $x=0$, 0.005, 0.02, and 0.03. We immediately note the overall equivalence, at least qualitatively, among the optical properties of the various alloys with different composition. As observed previously for FeSi,[19,33] we note the same progressive opening of a gap with decreasing temperature, leading to the suppression of spectral weight in the far- and mid-infrared range (FIR-MIR). The dc limit of $\sigma_1(\omega)$ at each temperature is consistent with the measured dc conductivity (see Sec. III A). For $x=0.02$ and 0.03 we do observe a residual metallic contribution to $\sigma_1(\omega)$ at low temperatures, which manifests itself by a constant $\sigma_1(\omega\rightarrow 0)\neq 0$ behavior below the FIR spectral range. This is distinctly different from the behavior of $\sigma_1(\omega)$ for $x=0$ and 0.005, where the metallic component cannot be resolved at low temperatures. We also note that the lost spectral weight due to the opening of the gap piles up at the gap absorption. Particularly for $x=0$, 0.005, and 0.02, $\sigma_1(\omega)$ at low temperatures displays peaks at $E_{\rm gap}$ exceeding the signal of the 300 K curve.[19,32]

However, for $x=0.03$ the gap feature is barely recognized and the transferred spectral weight does not induce a sizable peak in $\sigma_1(\omega)$. This is mainly the consequence of the higher reflectivity of the $x=0.03$ alloy in the FIR-MIR range. Nevertheless, the total spectral weight is fully recovered by $\omega<4\omega_{\rm gap}$ in all investigated alloys. Since no softening of the sharp phonon modes below the gap energy is observed, we conclude that the doping neither changes the electron-lattice coupling nor affects the symmetry of the crystal lattice, in agreement with previous x-ray and neutron scattering results.[11,13,14] In addition, their relative spectral weight or intensity remains unchanged.

The rather conventional and phenomenological approach, based on the classical Lorentz-Drude dispersion theory,[38] allows us to decouple the various contributions to $\sigma_1(\omega)$. For all compounds, we have assumed that $\sigma_1(\omega)$ can be described by a Drude term for the free charge carriers and a set of Lorentz harmonic oscillators for the phonon modes, the gap excitation, and the electronic interband transitions. For reasons of consistency, the number of harmonic oscillators has been kept constant for the different alloys. The fits reproduce the major features of the experimental results, namely, the progressive suppression of the Drude term with decreasing temperature, which is complete for $x=0$ and 0.005, and the rigidity of the phonon modes upon doping. These fits also serve for the reliable evaluation of the gap energy $E_{\rm gap}$. Its dependence on x is shown in Fig. 4. The comparison with the values extracted from the transport properties demonstrates that the gap is independent of x for $x\leqslant 0.02$ and tends to a 10–20% reduction for $x=0.03$. Considering the possible error bars in the evaluation procedures of the gap values from either dc transport or optical conductivity, we ascribe no significance to the slight difference between them.

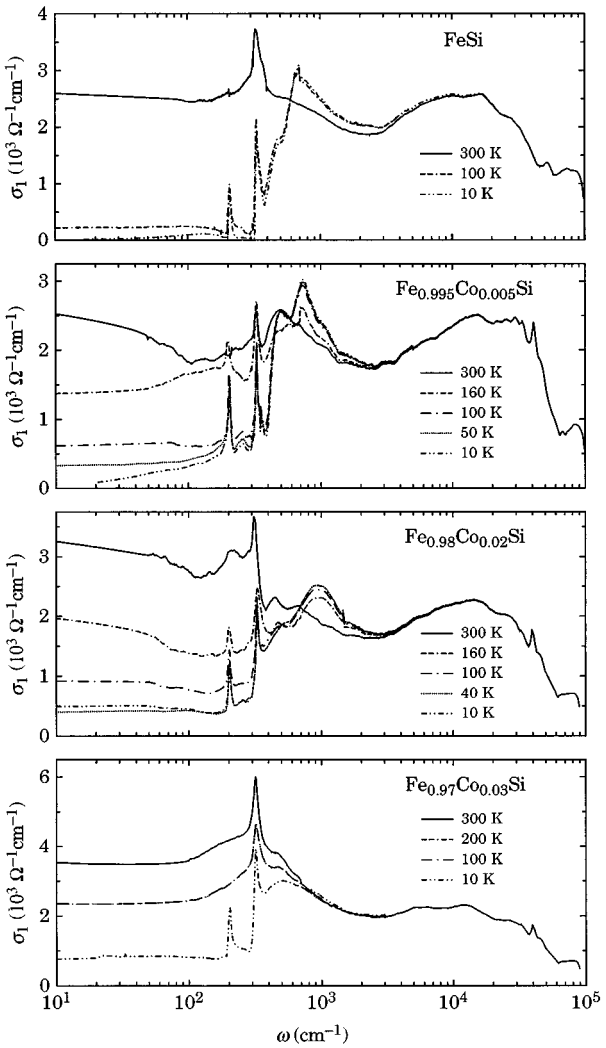

FIG. 10. Optical conductivity $\sigma_1(\omega)$ of $Fe_{1-x}Co_xSi$ with $x=0$, 0.005, 0.02, and 0.03 at fixed temperatures in the range between 10 and 300 K.

Finally, from the residual metallic component of $\sigma_1(\omega)$ at $T<10$ K for $x=0.02$ and 0.03, approximated with a Drude

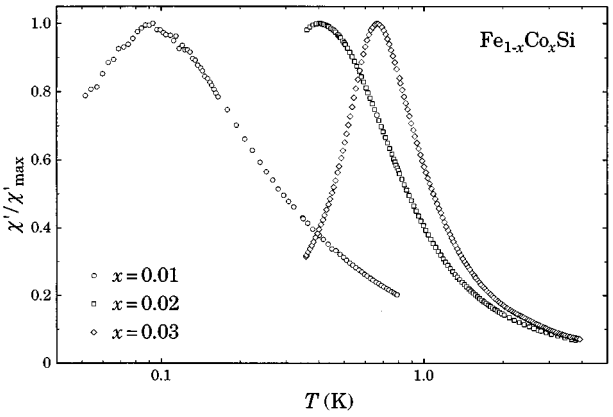

FIG. 11. Temperature variation of the real part $\chi'(T)$ of the complex ac magnetic susceptibility for the $Fe_{1-x}Co_xSi$ samples with $0.01 \leqslant x \leqslant 0.03$, below 4 K.

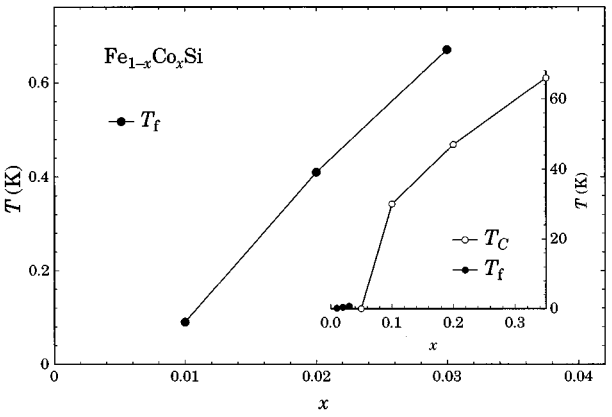

FIG. 12. Temperatures T_f at which the maxima in $\chi'(T)$ occur, as a function of Co concentration x. The inset shows the iron-rich part of the magnetic phase diagram of the $Fe_{1-x}Co_xSi$ system. Open circles: Curie temperatures T_C taken from Ref. 14; closed circles: the temperatures T_f. The lines are guides for the eye.

term, one may estimate the effective mass m^* and the concentration n of the itinerant charge carriers. This may be achieved by comparing the corresponding plasma frequency ω_p inferred from the fits, with the Sommerfeld $\gamma(T \to 0)$ value of the electronic contribution to the specific heat. With $\omega_p = 1832$ and 2652 cm^{-1} and $\gamma = 5.7$ and 7.6 mJ mol^{-1} K^{-2} (see Sec. III D) we obtain $m^*/m_e \sim 30$, with $n = 1.0 \times 10^{21}$ and 2.1×10^{21} cm^{-3} for $x = 0.02$ and 0.03, respectively. The latter numbers are consistent with additional charge carriers of the order of 1 electron per cobalt atom. For $x = 0$ and 0.005, the disappearance of the Drude component below 40 K prohibits this procedure. However, a simple linear extrapolation of ω_p for alloys with $x < 0.02$ and taking into account the corresponding γ values results again in a mass enhancement m^*/m_e of the order of 30. In this connection we note that cyclotron masses as high as $14.5 m_e$ have been deduced from the results of a study of the de Haas–van Alphen effect of MnSi, a weak itinerant ferromagnet with the $B20$ structure.[39]

C. Magnetic susceptibility

In Fig. 11 we show the real part $\chi'(T)$ of the complex ac magnetic susceptibility for the samples with $x = 0.01$, 0.02, and 0.03 between 0.05 and 4 K. In the same temperature range, the $\chi'(T)$ curve of nominally pure FeSi follows a Curie-Weiss-type law with a paramagnetic Curie temperature $\Theta = -0.036$ K and a very low value of the Curie constant. Well defined maxima in the χ' versus T plots appear at $T_f = 0.09$, 0.40, and 0.67 K for the alloys containing 1, 2, and 3 at % of cobalt, respectively, suggestive of a spin-glass-type freezing of magnetic moments. Since the appearance of the $\chi'(T)$ maxima occur at temperatures that increase with increasing x, this moment-freezing phenomenon is most likely related with the Co substitutions.

Above the respective temperatures T_f the χ' versus T variations can be well fitted using a Curie–Weiss-type law. The value of the effective moment per cobalt atom increases with increasing Co concentration. For the samples with $x = 0.02$ and 0.03, Θ is positive and of the order of T_f, indicating predominantly ferromagnetic interactions. On the contrary, for $Fe_{0.99}Co_{0.01}Si$, Θ is negative and of a much smaller absolute value than the corresponding T_f, indicating a trend towards weak antiferromagnetic coupling between magnetic moments. This sign change of the interaction may be related with a decrease of the characteristic length k_F^{-1} of the RKKY-type interaction with increasing carrier concentration. Here k_F is the Fermi wave vector, which, as our electrical conductivity results shown before in Sec. III A indicate, is expected to continuously increase with Co doping on the level of a few at %.

In Fig. 12 we plot the temperatures T_f at which the maxima in $\chi'(T)$ occur, as a function of cobalt concentration x. For comparison, in the inset of Fig. 12, we show the Curie temperatures T_C of $Fe_{1-x}Co_xSi$ with $x \geqslant 0.05$ taken from Ref. 14. The plots $T_f(x)$ and $T_C(x)$ imply that both the moment freezing and the onset of long-range magnetic order require that critical concentrations of Co doping are exceeded. The occurrence of a critical concentration of magnetic impurities for magnetic-moment freezing is characteristic of insulating spin glasses with short-range magnetic interaction.[40] On the other hand this is somewhat unusual for metallic spin glasses with long-range RKKY-type interaction. While our electrical conductivity $\sigma(T)$ results indicate that $Fe_{1-x}Co_xSi$ samples with $x \leqslant 0.01$ are metallic (see Sec. III A), the density of itinerant carriers may be insufficient to effectively mediate the magnetic interaction between the Co moments. We note surprisingly small values of T_f/x, which fall in the range between 9 and 22 K. Typical metallic spin glasses are characterized by much higher values of T_f/x, e.g., $T_f/x \approx 10^3$ K for $Au_{1-x}Fe_x$.[40] Values of T_f/x that are of similar magnitude to our results for $Fe_{1-x}Co_xSi$ have previously been reported for the spin-glass systems $La_{1-x}Gd_xAl_2$, $Y_{1-x}Gd_xAl_2$, and $La_{1-x}Gd_xB_6$, all with a weak exchange interaction between Gd moments, mediated by itinerant electrons.[41]

We have also measured $\chi'(T)$ curves near T_f for several excitation frequencies f in the range between 18 and 630 Hz. The χ' versus T maxima shift to higher temperatures with increasing frequency. Fitting the $T_f(f)$ data with a Vogel-Fulcher-type relation

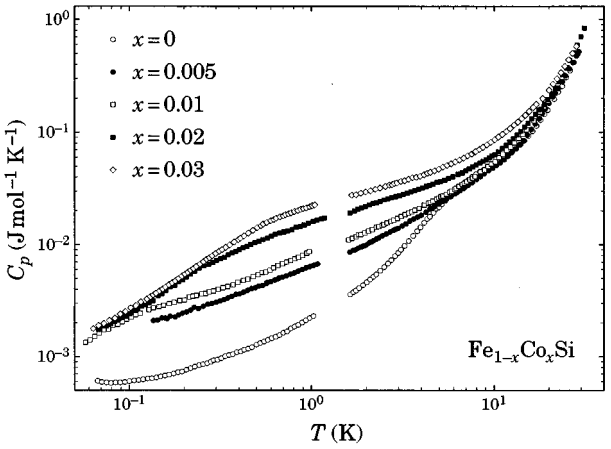

FIG. 13. Specific heat C_p of $Fe_{1-x}Co_xSi$ as a function of temperature between 0.06 and 30 K plotted on log-log scales.

$$\tau = \tau_0 \exp\left[\frac{E_a}{k_B(T_f - T_0)}\right] \tag{7}$$

and choosing $\tau_0 = 1\times10^{-13}$ s,[42] leads to values of T_0 that are substantially lower than the measured T_f values, indicating that the relaxation behavior is close to Arrhenius type. Arrhenius-type relaxations are characteristic of metallic spin glasses with a strongly reduced RKKY interaction and of insulating spin glasses with low concentrations of magnetic moments.[42] The observed type of relaxation is compatible with our evaluation of the very small values of T_f/x.

D. Specific heat

The complete set of the $C_p(T)$ data for all our samples of $Fe_{1-x}Co_xSi$, with the exception of $Fe_{0.9925}Co_{0.0075}Si$, in the temperature range between 0.06 and 30 K, is shown in Fig. 13. The same data, in the form of C_p/T versus T^2, are plotted in Fig. 14.

First we note a broad maximum in C_p/T of nominally pure FeSi centered at approximately 8.5 K, indicating a large excess specific heat $C_{ex}(T)$. The FeSi results between 1.5 and 30 K are very well fitted by the sum of contributions of the usual low-temperature electronic and lattice excitations and a Schottky anomaly resulting from excitations within a two-level system with a single interlevel energy Δ, i.e.,

$$C_p = \gamma T + \beta T^3 + \delta T^5 + A\left(\frac{\Delta}{k_B T}\right)^2 \times\left[1+\exp\left(\frac{\Delta}{k_B T}\right)\right]^{-2}\exp\left(\frac{\Delta}{k_B T}\right). \tag{8}$$

This fit is shown as a solid line through the data points of FeSi in Fig. 14. The Schottky anomaly is characterized by a level separation $\Delta \approx 2$ meV and an entropy release of 0.029 R at 30 K. This Schottky anomaly is distinctly smaller for the sample with $x=0.005$ and it cannot be identified in the $C_p(T)$ data for the samples with $x \geqslant 0.01$ (see Fig. 14). The fitting parameters γ, β, and δ for the two samples with $0 \leqslant x \leqslant 0.005$ are given in Table I.

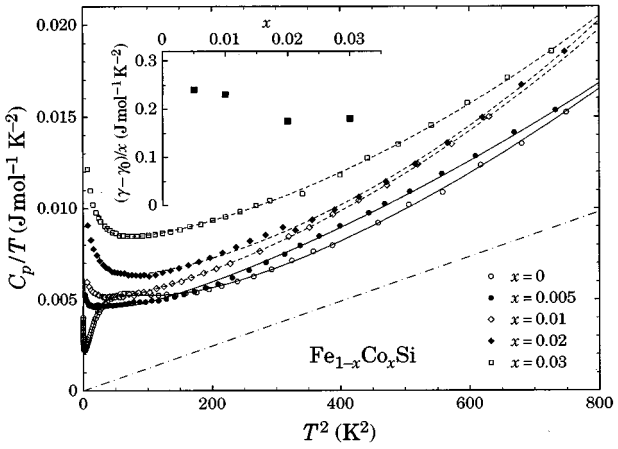

FIG. 14. C_p/T vs T^2 of $Fe_{1-x}Co_xSi$. The solid and dashed lines indicate the fits of Eqs. (8) and (11) to the C_p data for the samples with $x \leqslant 0.005$ and $x \geqslant 0.01$, respectively (see text). The dashed-dotted line indicates the Debye contribution of acoustic lattice excitations. Inset shows the difference $\gamma - \gamma_0$ between the coefficients of the linear terms to $C_p(T)$ of the cobalt-doped and pure FeSi, plotted as $(\gamma-\gamma_0)/x$ vs x.

In Fig. 14, we also show the expected acoustic phonon contribution for FeSi, which we have calculated from the results of low-temperature measurements of the elastic moduli c_{11}, c_{44} and $\frac{1}{2}(c_{11}-c_{12})$ (Ref. 34) using the Born–von Kármán formula for the average sound velocity v_s (Ref. 43)

$$\frac{3}{v_s^3} = \rho^{3/2}\left[\frac{2}{c_{44}^{3/2}} + \frac{1}{c_{11}^{3/2}} + \frac{3}{5}(c_{12}-c_{11}+2c_{44})\left(\frac{1}{c_{44}^{5/2}} - \frac{1}{c_{11}^{5/2}}\right)\right]. \tag{9}$$

Here ρ is the mass density. Equation (9) is valid for nearly isotropic cubic crystals, i.e., when the anisotropy parameter

$$\eta = \frac{c_{12}-c_{11}+2c_{44}}{c_{11}-c_{44}} \tag{10}$$

is small compared with unity. For FeSi $\eta = 0.21$, which indicates a fairly low elastic anisotropy of this material.

The ''elastic'' Debye temperature $\Theta_D^e = 341$ K that follows from the average sound velocity v_s obtained in the way described above is in good agreement with the ''thermodynamic'' Debye temperatures Θ_D^t of 369 and 357 K, which are compatible with the fitted values of the parameter β for our materials with $x=0$ and 0.005, respectively. In this connection we note that for various crystalline solids, including such different materials as elemental metals and ionic salts,

TABLE I. Parameters of the fits of Eq. (8) to the specific heat $C_p(T)$ data of $Fe_{1-x}Co_xSi$ with $x=0$ and 0.005 (see text).

x	γ, (mJ mol^{-1} K^{-2})	β, (μJ mol^{-1} K^{-4})	δ, (nJ mol^{-1}K^{-6})
0	2.2	9.7	9.9
0.005	3.4	10.7	7.7

TABLE II. Parameters of the fits of Eq. (11) to the specific heat $C_p(T)$ data of $Fe_{1-x}Co_xSi$ with $0.01 \leqslant x \leqslant 0.03$ (see text).

x	γ, (mJ mol^{-1} K^{-2})	B, (J mol^{-1} K)
0.01	4.5	0.07
0.02	5.7	0.20
0.03	7.6	0.24

the Debye temperatures Θ_D^t and Θ_D^e often differ by a few percent even if the latter is determined from low-temperature elastic-moduli data.[43–45]

For analyzing the $C_p(T)$ data of $Fe_{1-x}Co_xSi$ with $0.01 \leqslant x \leqslant 0.03$ at temperatures above 5 K, we recall that our $\chi'(T)$ results (Sec. III C) indicate these samples to exhibit a spin-glass-type freezing of magnetic moments below 1 K. Therefore, we assume that the main contributions to C_p are from electronic, lattice, and high-temperature spin-glass excitations, i.e.,

$$C_p = \gamma T + \beta T^3 + \delta T^5 + B T^{-2}. \tag{11}$$

The fits of the $C_p(T)$ data using Eq. (11) are shown as the dashed lines in Fig. 14. For materials with $x \geqslant 0.01$ a precise evaluation of the cubic term βT^3 meets difficulties because of the large magnetic contribution to the specific heat. The linear term γT, however, can reliably be determined as it appears to be rather insensitive to the details of the fitting procedure. The fitted values of γ and B for $Fe_{1-x}Co_xSi$ with $0.01 \leqslant x \leqslant 0.03$ are given in Table II.

For $Fe_{1-x}Co_xSi$, the coefficient γ of the linear term to the specific heat above 5 K increases with increasing doping level x (see Tables I and II). Interpreting the linear term γT of nominally pure FeSi as being due to an electronic density of states at the Fermi energy, we arrive at a surprisingly large electronic specific-heat parameter when considering the low concentration of itinerant carriers, as implied by our electrical conductivity $\sigma(T)$ results described in Sec. III A. For cobalt-doped materials, the assumption that the difference $(\gamma - \gamma_0)T$ between the linear terms to $C_p(T)$ of doped and pure FeSi corresponds to one itinerant electron per cobalt impurity, leads to an average value of $(\gamma - \gamma_0)/x$ of 0.2 J mol^{-1} K^{-2}, suggestive of a considerable enhancement of the effective mass (see inset of Fig. 14). This implies that at low temperatures the Fermi level resides in a partially filled narrow band—a rather unusual scenario for a 3*d* transition-metal system.

For $Fe_{1-x}Co_xSi$ with $x \geqslant 0.02$, the magnetic contribution $C_m(T)$ to the total measured specific heat $C_p(T)$, obtained by subtracting off the estimates of the electronic and the lattice terms, exhibits broad maxima at temperatures that are distinctly higher than the respective freezing temperatures T_f. This observation is consistent with our conjecture of a spin-glass-type freezing of magnetic moments in these materials because in spin glasses a substantial difference between T_f and the temperature of the maximum in $C_p(T)$ has often been observed.[40] The magnetic entropy ΔS_m, obtained from the magnetic specific heat C_m via

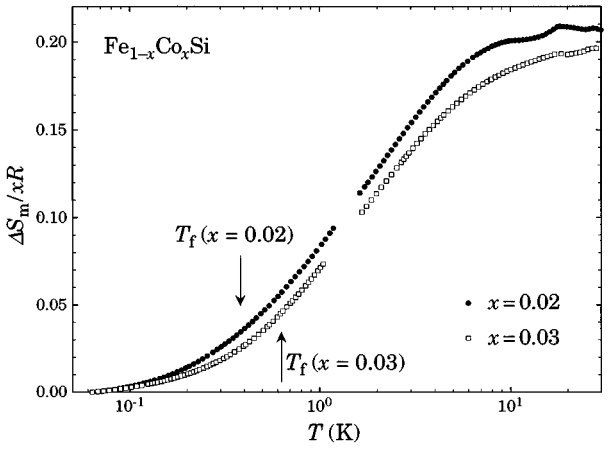

FIG. 15. Magnetic entropy ΔS_m of $Fe_{1-x}Co_xSi$ with $x = 0.02$ and 0.03 plotted as $\Delta S_m/x$ vs T, below 30 K.

$$\Delta S_m(T) = \int_{T_0}^{T} \frac{C_m}{T'} dT', \tag{12}$$

saturates at 30 K reaching $\approx 0.20R$ per mole of Co (see Fig. 15). The magnetic entropy released below T_f removes only about 18 and 25% of the saturation value of ΔS_m for materials with $x = 0.02$ and 0.03, respectively. This implies a considerable short-range order above T_f, which is a common feature of spin glasses.[40]

IV. CONCLUSIONS

The electrical conductivity, the optical reflectivity, the ac magnetic susceptibility, and the specific heat of $Fe_{1-x}Co_xSi$ with $0 \leqslant x \leqslant 0.03$ have been measured in varying temperature ranges between 0.05 K and 300 K. Our electrical conductivity data imply that FeSi is an impure hybridization-gap semiconductor ($E_{gap} \approx 80$ meV) at moderate temperatures but enters a semimetallic state with a very small number of itinerant carriers below 0.1 K. The $T^{1/2}$ variation of the electrical conductivity σ of $Fe_{1-x}Co_xSi$ with $x = 0.02$ and 0.03 below 0.5 K indicates that the temperature dependence of σ of these materials close to $T = 0$ is dominated by the diffusion-channel term arising from Coulomb interaction among itinerant electrons. The optical data confirm both the magnitude of the gap and the trend to its slight reduction for the alloy with 3 at% Co content.

For $Fe_{1-x}Co_xSi$ with $x \geqslant 0.01$, a spin-glass-type freezing of magnetic moments is observed between 0.09 and 0.7 K. The small values of T_f/x and the $T_f(f)$ variations are both indicative of a weak interaction among the moments. Upon reducing the cobalt concentration x, this interaction changes from ferromagnetic to antiferromagnetic in the range $0.01 \leqslant x \leqslant 0.02$. This crossover is accompanied by a decrease of T_f/x by a factor of 2 leading to a concave down variation of T_f versus x.

The specific heat $C_p(T)$ of $Fe_{1-x}Co_xSi$ contains a term γT that increases with increasing x from $2.1T$ mJ mol^{-1}

K^{-1} for FeSi to $7.6T$ mJ mol^{-1} K^{-1} for $Fe_{0.97}Co_{0.03}Si$. Assuming that the difference $(\gamma-\gamma_0)T$ between the linear terms of $C_p(T)$ of doped and pure FeSi is due to an additional electronic DOS at the Fermi energy and that this DOS corresponds to one itinerant electron per cobalt impurity, leads to values of $(\gamma-\gamma_0)/x$ reaching 0.24 J mol^{-1} K^{-2}, indicating a considerable enhancement of the effective mass. The numerical estimate of the mass enhancement using optical and specific-heat data, as explained in Sec. III B, gives $m^*/m_e \sim 30$, a surprisingly high value for 3*d* transition-metal alloys. Thus the low-temperature state of FeSi is that of a strongly correlated metal with a very low concentration of itinerant charge carriers, again a rather unusual feature for a 3*d* transition-metal compound.

ACKNOWLEDGMENTS

We gratefully acknowledge useful discussions with R. Monnier. We thank M. Hunt and K. Iliadis for doing electrical-resistivity measurements at an early stage of this work, and J. Müller for technical assistance. One of us (L.D.) is particularly grateful to P. Wachter for generously providing infrastructural support. This work was in part financially supported by the Schweizerische Nationalfonds zur Förderung der wissenschaftlichen Forschung.

*Present address: Oak Ridge National Laboratory, Oak Ridge, Tennessee 37831.

[1] G. Aeppli and Z. Fisk, Comments Condens. Matter Phys. **16**, 155 (1992).
[2] V. Jaccarino, G. K. Wertheim, J. H. Wernick, L. R. Walker, and S. Arajs, Phys. Rev. **160**, 476 (1967).
[3] M. B. Hunt, M. A. Chernikov, E. Felder, H. R. Ott, Z. Fisk, and P. Canfield, Phys. Rev. B **50**, 14 933 (1994).
[4] P. Lunkenheimer, G. Knebel, R. Viana, and A. Loidl, Solid State Commun. **93**, 891 (1995).
[5] S. Paschen, E. Felder, M. A. Chernikov, H. R. Ott, J. L. Sarrao, and Z. Fisk, Czech. J. Phys. **46**, 1997 (1996).
[6] H. Watanabe, Y. Yamamoto, and K. Ito, J. Phys. Soc. Jpn. **18**, 995 (1963).
[7] L. F. Mattheiss and D. R. Hamann, Phys. Rev. B **47**, 13 114 (1993).
[8] C. Fu, M. P. C. M. Krijn, and S. Doniach, Phys. Rev. B **49**, 2219 (1994).
[9] M. J. Rozenberg, G. Kotliar, and H. Kajueter, Phys. Rev. B **54**, 8452 (1996).
[10] D. Mandrus, J. L. Sarrao, A. Migliori, J. D. Thompson, and Z. Fisk, Phys. Rev. B **51**, 4763 (1995).
[11] L. F. Romasheva, R. P. Krentsis, and P. V. Gel'd, Fiz. Tverd. Tela (Leningrad) **22**, 621 (1980) [Sov. Phys. Solid State **22**, 365 (1980)].
[12] A. Lacerda, H. Zhang, P. C. Canfield, M. F. Hundley, Z. Fisk, J. D. Thompson, C. L. Seaman, M. B. Maple, and G. Aeppli, Physica B **186-188**, 1043 (1993).
[13] J. Beille, J. Voiron, F. Towfiq, M. Roth, and Z. Y. Zhang, J. Phys. F **11**, 2153 (1981).
[14] J. Beille, J. Voiron, and M. Roth, Solid State Commun. **47**, 399 (1983).
[15] K. Ishimoto, Y. Yamaguchi, S. Mitsuda, M. Ishida, and Y. Endoh, J. Magn. Magn. Mater. **54-57**, 1003 (1986).
[16] K. Ishikawa, K. Tajima, D. Bloch, and M. Roth, Solid State Commun. **19**, 525 (1976).
[17] T. Ericsson, W. Karner, L. Häggström, and K. Chandra, Phys. Scr. **23**, 1118 (1981).
[18] M. Hansen and K. Anderko, *Constitution of Binary Alloys* (McGraw-Hill, New York, 1958), p. 714.
[19] L. Degiorgi, M. Hunt, H. R. Ott, M. Dressel, B. J. Feenstra, G. Grüner, Z. Fisk, and P. Canfield, Europhys. Lett. **28**, 341 (1994).
[20] B. C. Sales, E. C. Jones, B. C. Chakoumakos, J. A. Fernandez-Baca, H. E. Harmon, J. W. Sharp, and E. H. Volckmann, Phys. Rev. B **50**, 8207 (1994).
[21] C.-H. Park, Z.-X. Shen, A. G. Loeser, D. S. Dessau, D. G. Mandrus, A. Migliori, J. L. Sarrao, and Z. Fisk, Phys. Rev. B **52**, 16 981 (1995).
[22] T. Saitoh, A. Sekiyama, T. Mizokawa, A. Fujimori, K. Ito, H. Nakamura, and M. Shiga, Solid State Commun. **95**, 307 (1995).
[23] S. Takagi, H. Yasuoka, S. Ogawa, and J. H. Wernick, J. Phys. Soc. Jpn. **50**, 2539 (1981).
[24] N. F. Mott, J. Non-Cryst. Solids **1**, 1 (1968).
[25] T. F. Rosenbaum, R. F. Milligan, M. A. Paalanen, G. A. Thomas, R. N. Blatt, and W. Lin, Phys. Rev. B **27**, 7509 (1983).
[26] A. L. Efros and B. I. Shklovskii, J. Phys. C **8**, L49 (1975).
[27] A. I. Efros, J. Phys. C **9**, 202 (1976).
[28] A. Möbius, Solid State Commun. **73**, 215 (1990).
[29] M. Pollak, Philos. Mag. B **42**, 781 (1980); J. Non-Cryst. Solids **35-36**, 83 (1980).
[30] B. L. Altshuler and A. G. Aronov, in *Electron-Electron Interactions in Disordered Systems*, edited by V. M. Agranovich and A. A. Maradudin (North-Holland, Amsterdam, 1985), p. 690.
[31] N. F. Mott, Philos. Mag. B **44**, 265 (1981).
[32] S. Paschen, E. Felder, M. A. Chernikov, H. R. Ott, D. P. Young, J. L. Sarrao, and Z. Fisk (private communication).
[33] Z. Schlesinger, Z. Fisk, Hai-Tao Zhang, M. B. Maple, J. F. DiTusa, and G. Aeppli, Phys. Rev. Lett. **71**, 1748 (1993).
[34] J. L. Sarrao, D. Mandrus, A. Migliori, Z. Fisk, and E. Bucher, Physica B **199-200**, 478 (1994).
[35] P. Nyhus, S. L. Cooper, and Z. Fisk, Phys. Rev. B **51**, 15 626 (1995).
[36] J. Aarts and A. P. Volodin, Physica B **206-207**, 43 (1995).
[37] H. Fritzsche, in *The Metal–Non-Metal Transition in Disordered Systems*, edited by L. R. Friedman and D. P. Tunstall (SUSSP Publ., Edinburgh, 1978), p. 193.
[38] F. Wooten, *Optical Properties of Solids* (Academic Press, New York, 1972).
[39] L. Taillefer and G. G. Lonzarich, J. Magn. Magn. Mater. **54-57**, 957 (1986).
[40] K. Binder and A. P. Young, Rev. Mod. Phys. **58**, 811 (1986).
[41] J. Aarts, W. Felsch, H. v. Löhneysen, and F. Steglich, Z. Phys. B **40**, 127 (1980).
[42] J.-L. Tholence, Solid State Commun. **35**, 113 (1980).
[43] M. Blackman, Rep. Prog. Phys. **8**, 11 (1941).
[44] G. A. Alers and J. R. Neighbours, Rev. Mod. Phys. **31**, 675 (1959).
[45] K. Gschneider, in *Solid State Physics. Advances and Applications*, Vol. 16, edited by F. Seitz and D. Turnbull (Academic Press, New York, 1964), p. 275.